

Supporting information

Building an In-rich interphase to stabilize lithium metal anodes with a solid-like electrolyte

Jiashuai Li, Dongze Li, Qiufen Li, Mengxi Bai, Xiang Wang, Xiaoyan Lin, Siyuan Shao, and Ziqi Wang*

Department of Materials Science and Engineering, College of Chemistry and Materials Science, Jinan University, Guangzhou 511443, P. R. China

AUTHOR INFORMATION

Corresponding Author

Z.W.* wangzq@jnu.edu.cn

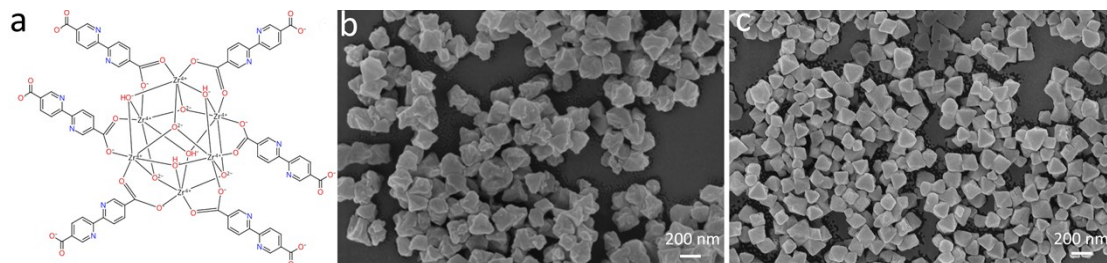


Fig. S1. (a) Structural formula of MOF-867. SEM images of the as-prepared (a) MOF-867 and (b) In-MOF.

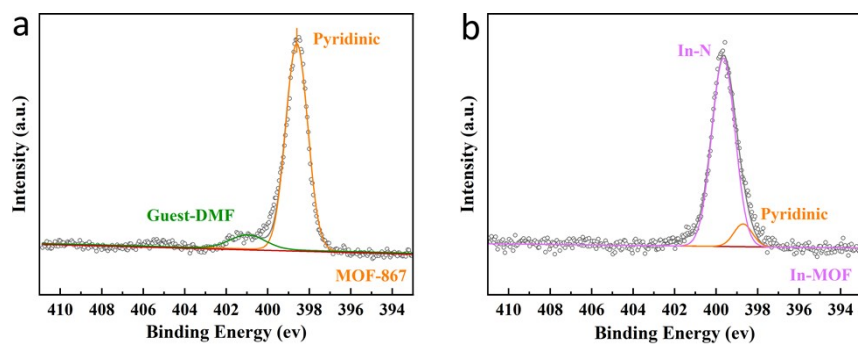


Fig. S2. The N 1s XPS spectra of (a) MOF-867 and (b) In-MOF.

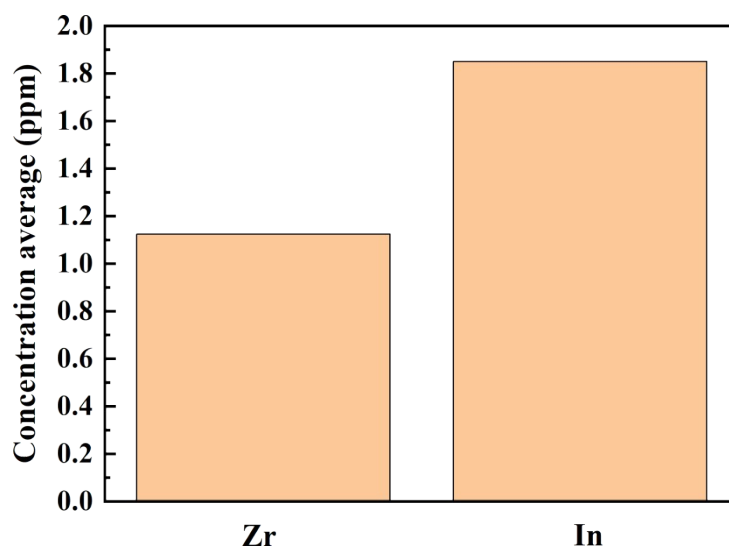


Fig. S3. Average Zr and In concentrations in ICP assays.

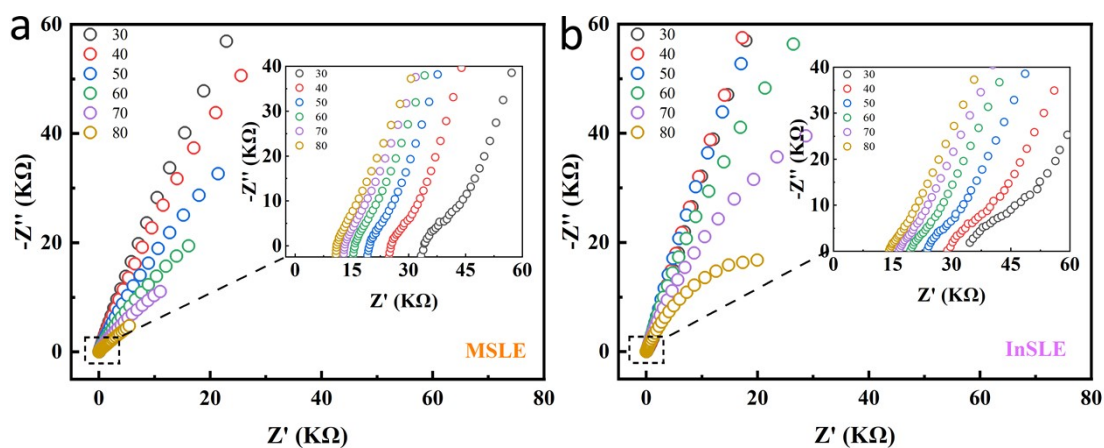


Fig. S4. The EIS spectra of the two MOF-based SLEs at different temperatures.

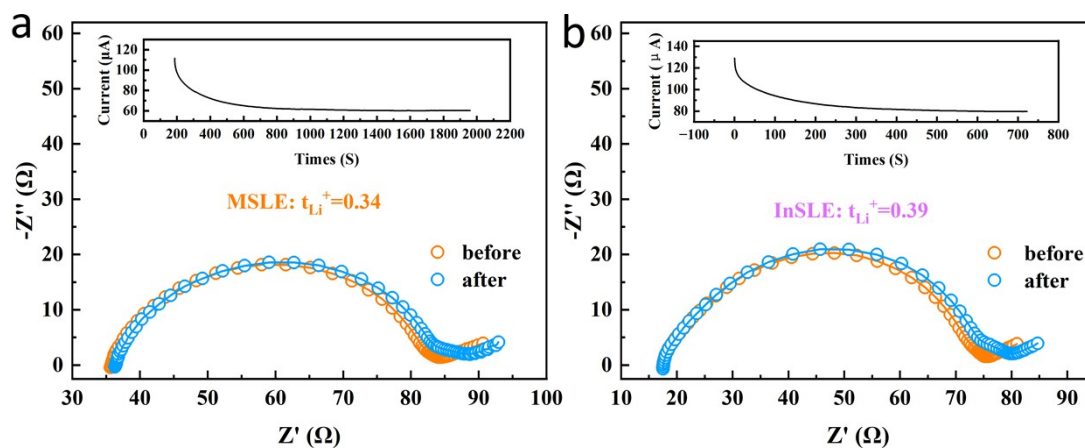


Fig. S5. The test for the t_{Li}^+ of (a) MSLE and (b) InSLE.

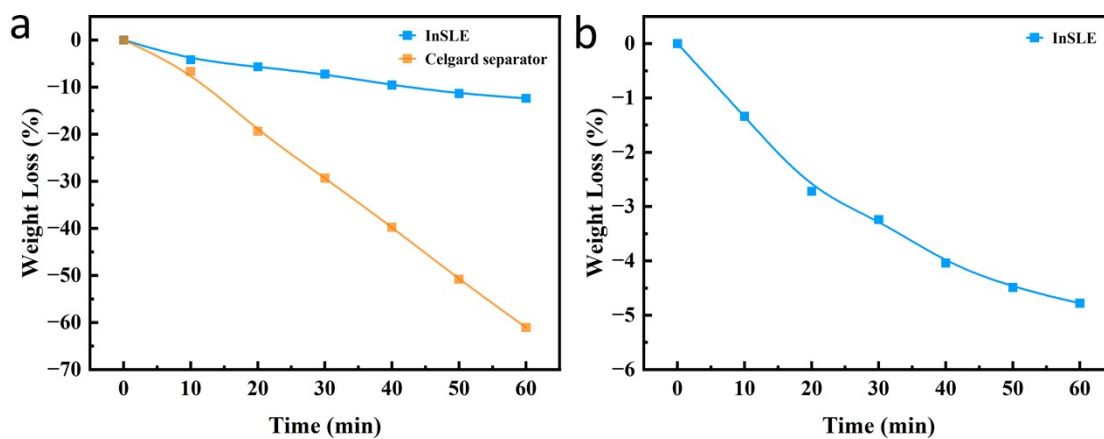


Fig. S6. Weight loss of the InSLE and the Celgard separator absorbed with $30 \mu\text{l}$ PC electrolyte at (a) 40°C and (b) room temperature.

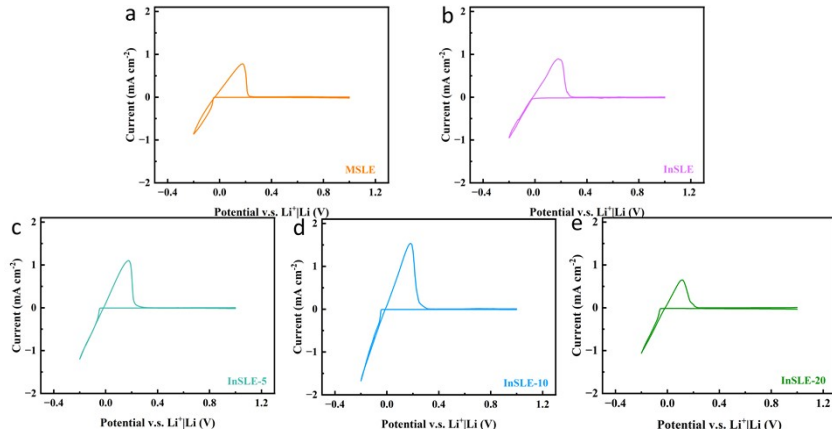


Fig. S7. CV profiles of the (a) MSLE, (b) InSLE (c) InSLE-5, (d) InSLE-10 and (e) InSLE-20 symmetric cells at a scan speed of 0.2 mV s⁻¹.

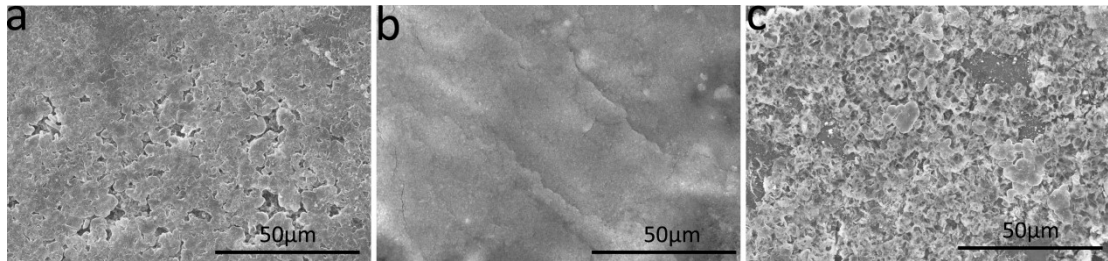


Fig. S8. SEM morphologies of the Li metal anodes after 20 cycles of plating/stripping tests with the (a) MSLE, (b) InSLE-10 and (c) InSLE electrolytes.

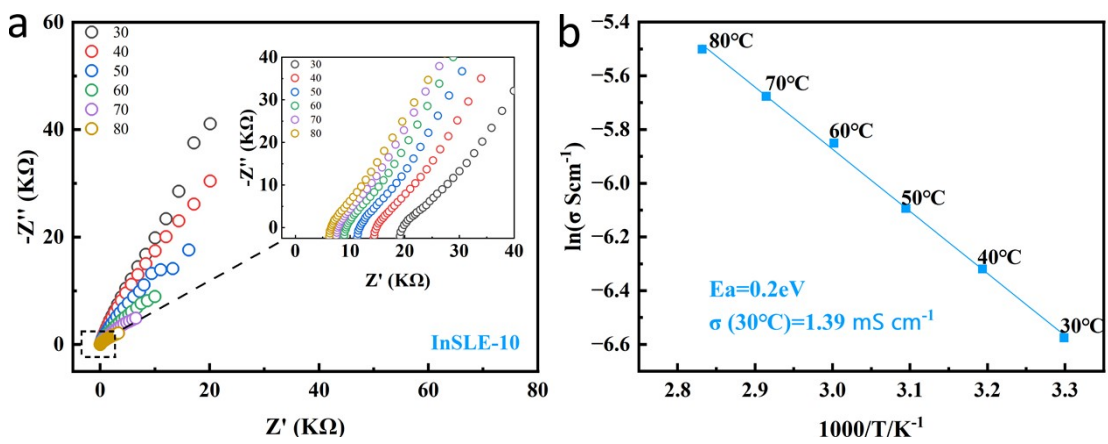


Fig. S9. (a) The EIS spectra of the InSLE-10 at different temperatures. (b) Arrhenius plot for the ionic conductivity of InSLE-10.

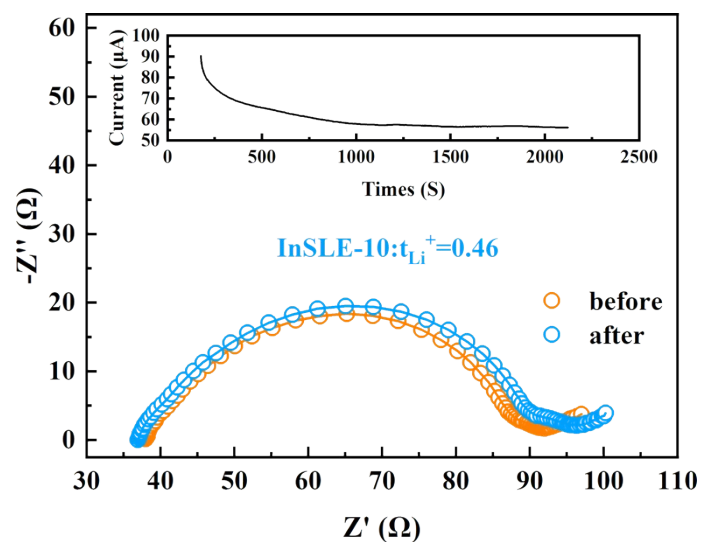


Fig. S10. The test for the t_{Li^+} of InSLE-10.

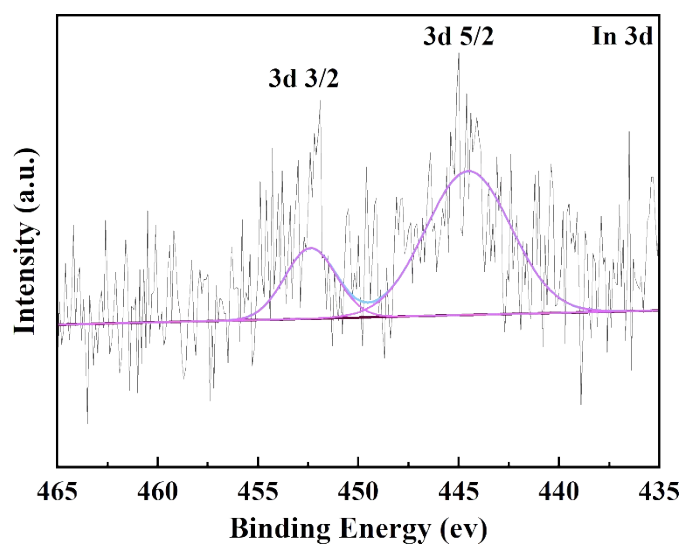


Fig. S11. The XPS In 3d spectra of the deposited Li with InSLE-10.

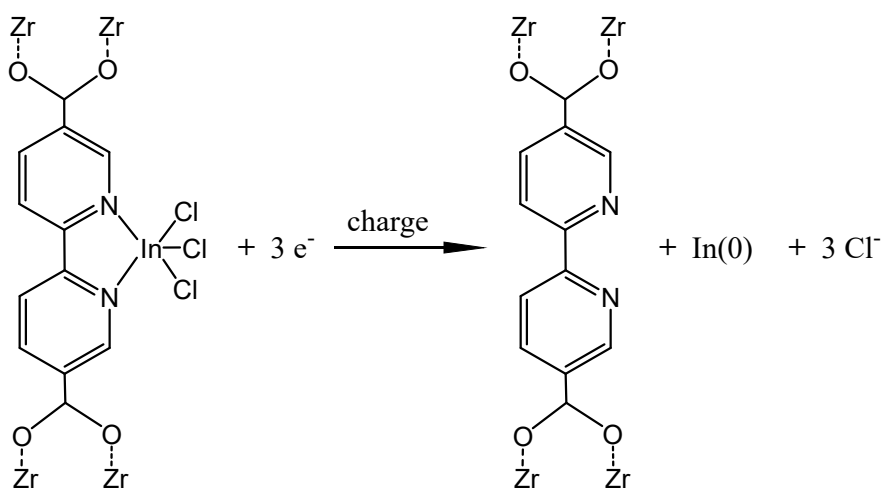


Fig. S12. The proposed mechanism for the formation of the In-rich SEI.

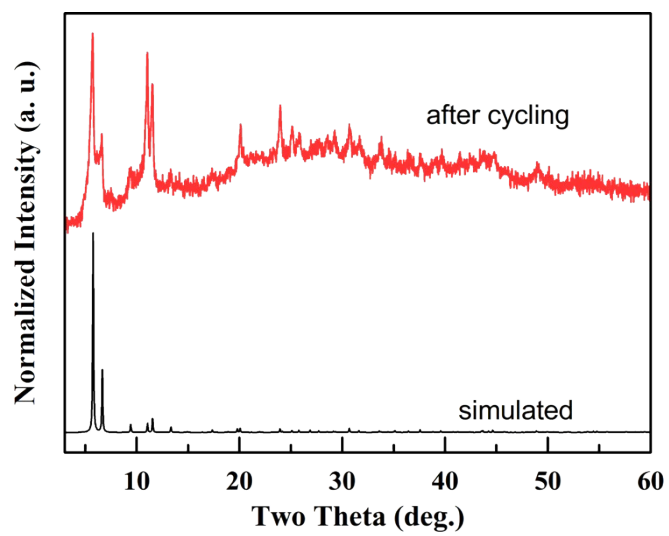


Fig. S13. XRD patterns of the SLE after plating/stripping cycling.

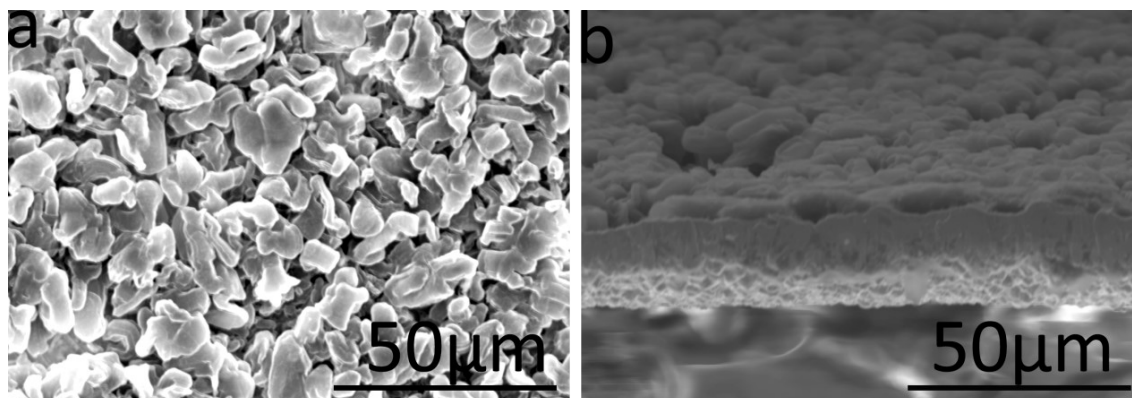


Fig. S14. SEM morphologies of the deposited Li (0.1 mA cm^{-2} , 1.0 mAh cm^{-2}) with the InSLE. (a) Top view. (b) Cross-section view.

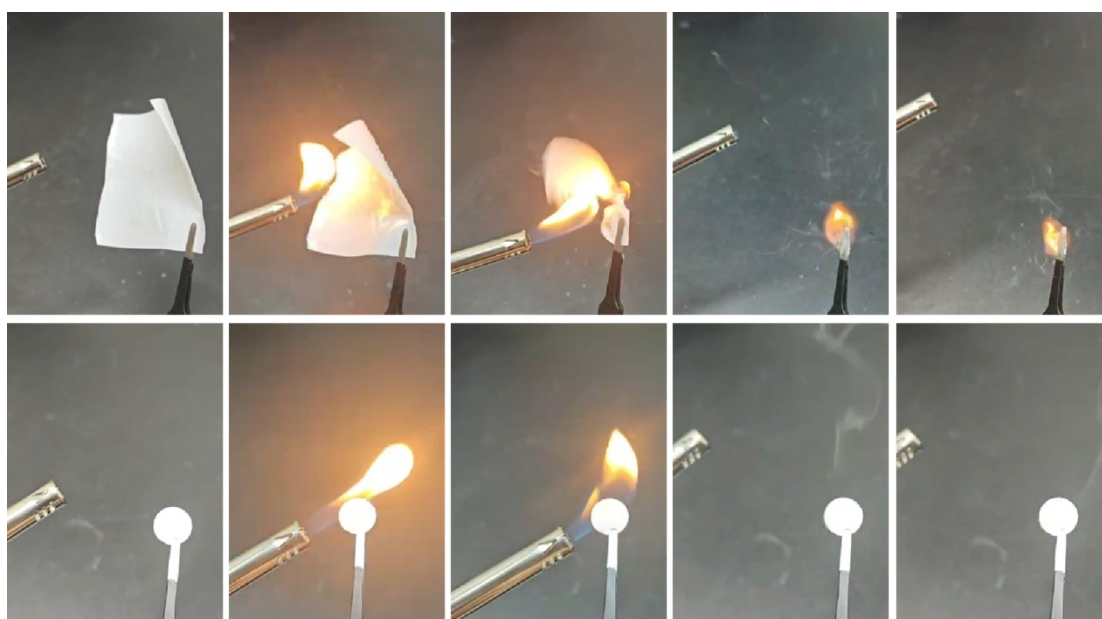


Fig. S15. Snapshots taken when the liquid PC electrolyte (on a Celgard separator, top) and the SLE (bottom) were exposed to the flame.

Table S1. Performance comparison of the reported LFP cells using MOF-based electrolytes.

Materials	Cathodes	Specific Capacity (mAh g ⁻¹)	Cycle number	Charge/discharge rate	Refs.
PEO/HKUST-1/LLZO/LiTFSI	LFP	160	400	0.1 C@50°C	1
HKUST/PIN	LFP	150	100	0.1 C@25°C	2
NiCo-MOF/SN	LFP	159	200	0.2 C@25°C	3
UiO-67/PVDF-HFP/ PVB	LFP	156	200	0.1 C@60°C	4
ZIF-8/PEO/LiTFSI	LFP	159	100	0.1 C@30°C	5
Zn-MOF-74/LiTFSI	LFP	152	100	0.1 C@30°C	6
UiO-66-NH ₂ -LIM/Li-IL	LFP	160	200	0.1 C@25°C	7
UiO-66-NH-M/AIBN	LFP	155	200	0.2 C@25°C	8
UIO-66/SILs	LFP	160	100	0.1 C@25°C	9
ZIF-8/PEO/LiClO ₄	LFP	160	120	0.1 C@25°C	10
InSLE-10	LFP	165	480	0.1 C@32°C	This work

References

- 1 M. Zhang, A. Yusuf and D.-Y. Wang, *J. Power Sources*, 2024, **591**, 233812.
- 2 X. Tian, Y. Yi, Z. Wu, G. Cheng, S. Zheng, B. Fang, T. Wang, D. G. Shchukin, F. Hai, J. Guo and M. Li, *Chem. Eng. Sci.*, 2023, **266**, 118271.
- 3 T. Zhao, W. Kou, Y. Zhang, W. Wu, W. Li and J. Wang, *J. Power Sources*, 2023, **554**, 232349.
- 4 Q. Zhang, T. Wei, J. Lu, C. Sun, Y. Zhou, M. Wang, Y. Liu, B. Xiao, X. Qiu and S. Xu, *J.*

- Electroanal. Chem.*, 2022, **926**, 116935.
- 5 C. Li, S. Deng, W. Feng, Y. Cao, J. Bai, X. Tian, Y. Dong and F. Xia, *Small*, 2023, **19**, 2300066.
- 6 P. Dong, X. Zhang, W. Hiscox, J. Liu, J. Zamora, X. Li, M. Su, Q. Zhang, X. Guo, J. McCloy and M.-K. Song, *Adv. Mater.*, 2023, **35**, 2211841.
- 7 Z. Wu, Y. Yi, F. Hai, X. Tian, S. Zheng, J. Guo, W. Tang, W. Hua and M. Li, *ACS Appl. Mater. Interfaces*, 2023, **15**, 22065.
- 8 W. Shang, Y. Chen, J. Han, P. Ouyang, C. Fang and J. Du, *ACS Appl. Energ. Mater.*, 2020, **3**, 12351.
- 9 Z. Liu, Z. Hu, X. Jiang, X. Wang, Z. Li, Z. Chen, Y. Zhang and S. Zhang, *Small*, 2022, **18**, 2203011.
- 10 Y. Xia, N. Xu, L. Du, Y. Cheng, S. Lei, S. Li, X. Liao, W. Shi, L. Xu and L. Mai, *ACS Appl. Mater. Interfaces*, 2020, **12**, 22930.